Thesis Proposal: Nanostructures with Topological Insulators

Mahmoud Lababidi

December 13, 2011

Introduction

Introduction

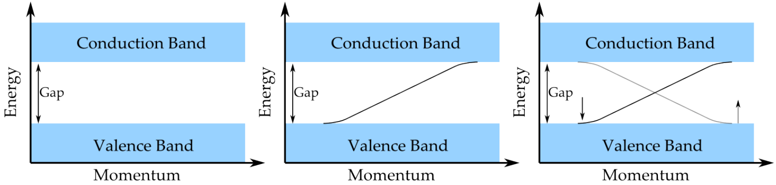

(a) Energy spectrum of a trivial band insulator
(b) Energy spectrum of a quantum hall state
(c) Energy spectrum of a topological insulator

Introduction

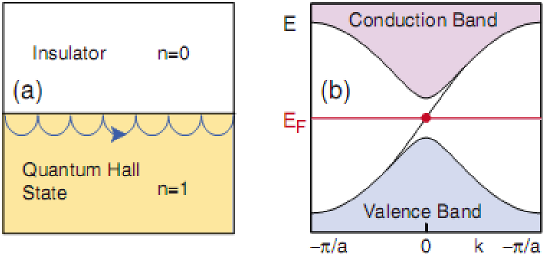

Introduction

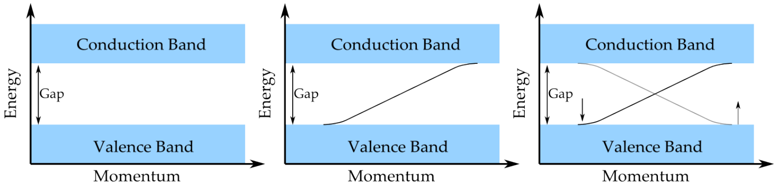

(a) Energy spectrum of a trivial band insulator
(b) Energy spectrum of a quantum hall state
(c) Energy spectrum of a topological insulator

Introduction

$$E = \pm(k^2 - M)$$

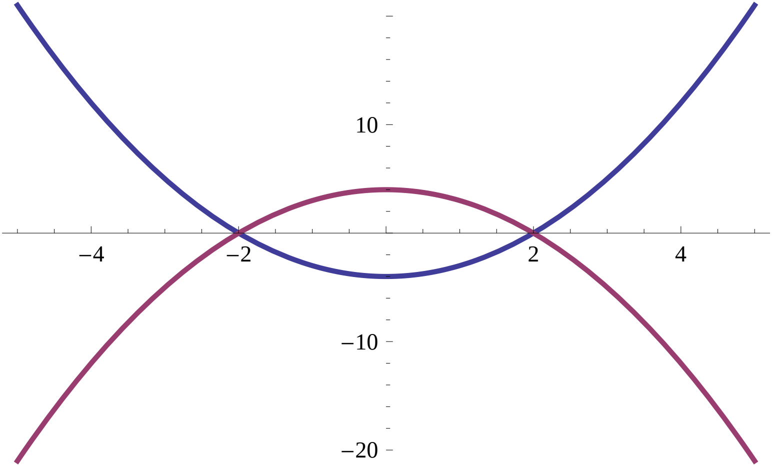

Introduction

$$E = \pm\sqrt{(k^2 - M)^2}$$

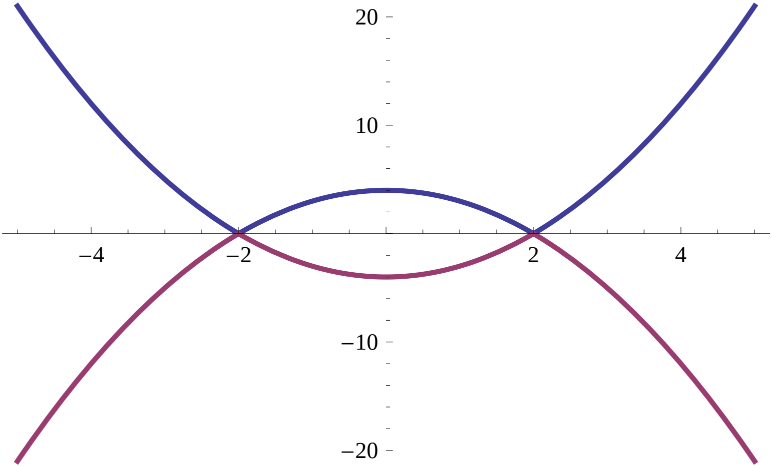

Introduction

$$E = \pm\sqrt{(k^2 - M)^2 + \alpha k^2} \text{ (spin-orbit)}$$

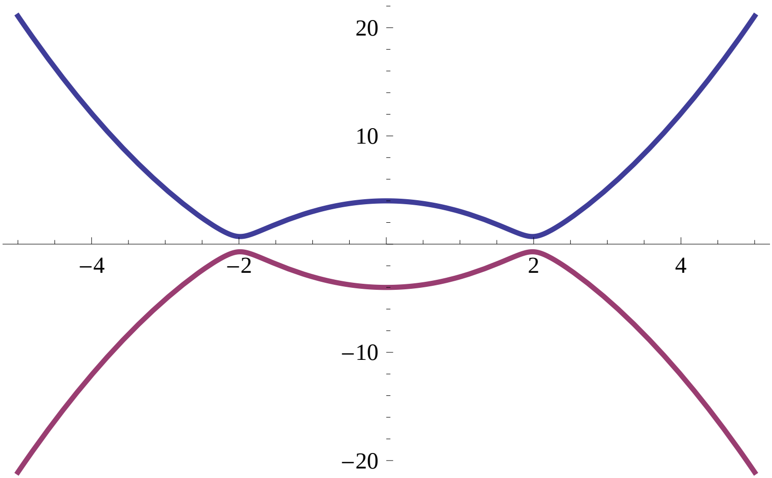

Introduction

How do we get the connecting state between the valence band to the conduction band?

Introduction

Let's try adding a boundary!

Introduction

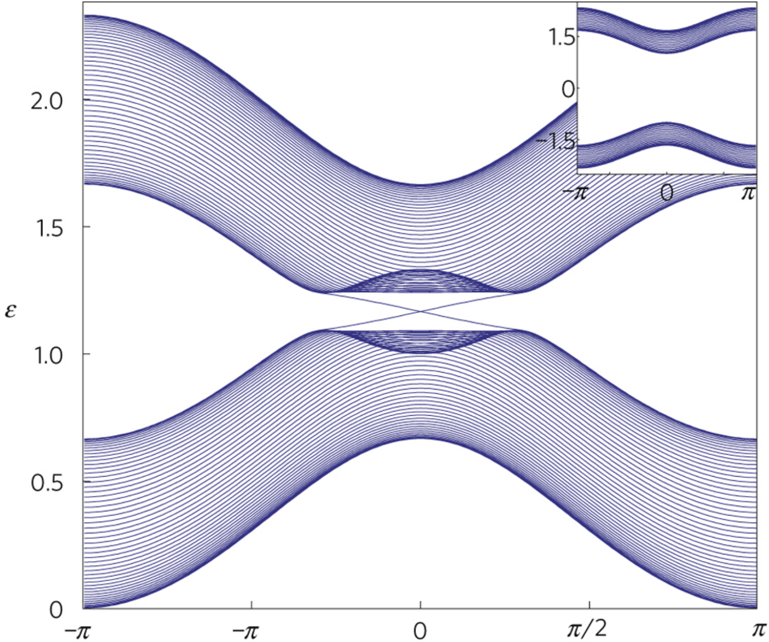

Introduction

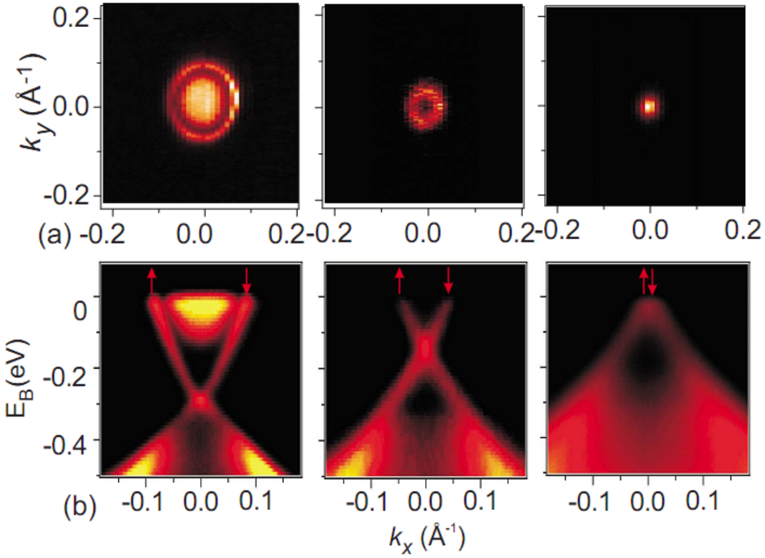

Motivation and Background

Insulating bulk with metallic surface states.
Surface Dirac Fermions which behave relativistically and zero mass
Dispersion: $E = \pm\hbar v k$
Surface Hamiltonian

$$H = \hbar v \vec{\sigma} \cdot \vec{k} - \mu = \hbar v(\sigma_x k_x + \sigma_y k_y) - \mu$$

σ are the Pauli spin matrices, μ is the chemical potential.

Applications

Electronics & Spintronics
Majorana Particles
$\rightarrow$Topological Quantum Computation
Topological order
Klein Tunneling

Metal to TI Scattering

What is the physics of an electron scattering off of a TI surface?

Metal to TI Scattering

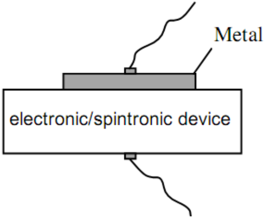

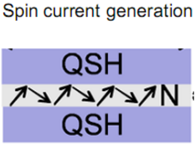

Yokoyama et al,
PRL 102, 166801(2009)

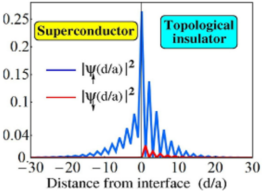

Stanescu et al,
PRB 81, 241310 (2010)

Metal to TI Scattering

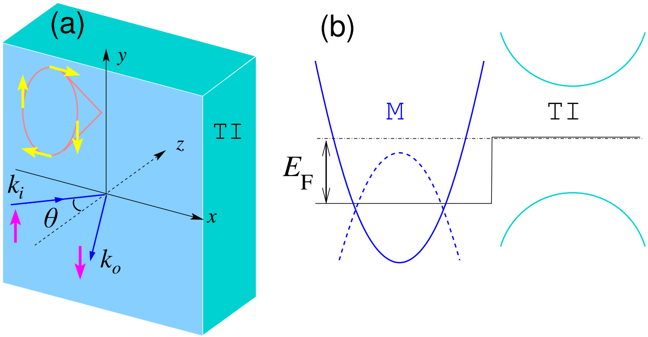

(a) Scattering geometry at a metal (M)-topological insulator (TI) interface.
(b) Schematic band structure of the metal (modeled by $\hat{H}_M$) and topological insulator.

Metal to TI Scattering

The scattering (reflection) matrix has the form

$$\hat{S}(\mathbf{k}) = \begin{pmatrix} g & \bar{f} \\ f & \bar{g} \end{pmatrix},$$

where $|g|^2 + |f|^2 = 1$ and $\alpha = \mathrm{Arg}(g^* f)$
The wave function inside the metal ($z < 0$):

$$\hat{\Phi}_M = (r_1 e^{-ik'_z z}, r_2 e^{-ik'_z z}, e^{ik_z z} + g e^{-ik_z z}, f e^{-ik_z z})^{\mathrm{T}},$$

Ben-Daniel and Duke boundary condition:

$$\hat{\Phi}_M = \hat{\Phi}_{TI}, \quad \hat{v}_M \hat{\Phi}_M = \hat{v}_{TI} \hat{\Phi}_{TI}.$$

velocity matrix $\hat{v}_i = \partial \hat{H}_i / \partial k_z$, $i \in \{M, TI\}$.

Metal to TI Scattering

The magnitudes (upper panel) and the phases (lower panel) of the spin-flip amplitude f and spin-conserving amplitude g versus the incident angle θ. $E = 0.1$eV, E_F=0.28eV. $|g|^2 + |f|^2 = 1$.

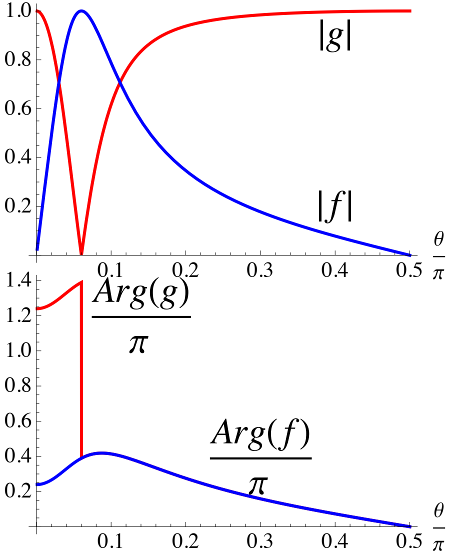

Metal to TI Scattering

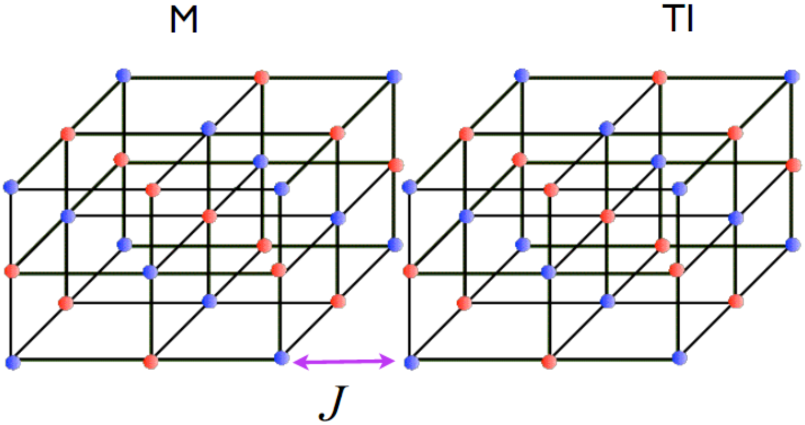

Metal to TI Scattering: Spectral Function

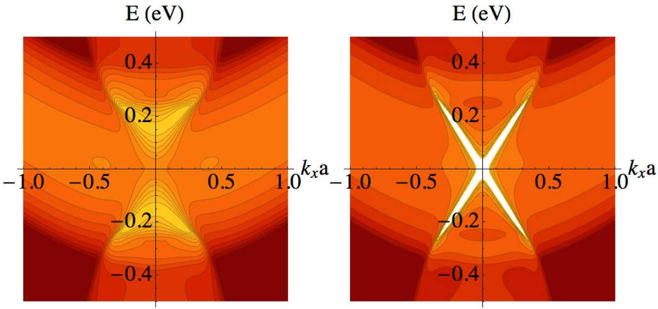

The spectral function $N(E, k_x, k_y = 0)$ at the interface of M-TI
Left: good contact, $J = t_M$, showing the continuum of MIGS.
Right: poor contact, $J = 0.2t_M$ showing Dirac spectrum
$t_M = 0.18eV$, $\mu_M = -4t_M$, a is lattice spacing.

Metal to TI Scattering

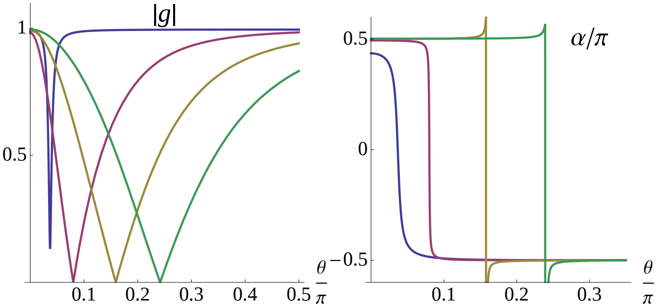

$J/t_M = 0.25, 1, 1.5, 2$ (from left to right). $t_M = 0.18eV$, $\mu_M = -4t_M$, $E = 0.05$eV, $k_y = 0$.

Metal to TI Scattering

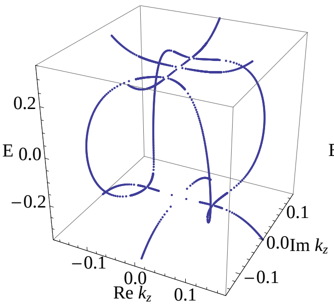

Figure: The complex band structure of topological insulator described by $\hat{H}_{TI}(\mathbf{k})$ for $k_y = 0$, $k_x = 0.02$ (left) and 0.04 (right). E is measured in eV, and k in $\AA^{-1}$. Subgap states with complex k_z represent evanescent waves. The topology of real lines [**?**] changes as k_x is increased.

Metal to TI Scattering: Summary

* Critical incident angle at which complete (100%) spin flip reflection
* Well-defined Dirac cone in the tunneling limit
* Good contacts: metal induced gap states

Next

Onto superconducting proximity effect...

The Fu-Kane Proposal

PRL **100**, 096407 (2008) PHYSICAL REVIEW LETTERS week ending 7 MARCH 2008

Superconducting Proximity Effect and Majorana Fermions at the Surface of a Topological Insulator

Liang Fu and C. L. Kane

Department of Physics and Astronomy, University of Pennsylvania, Philadelphia, Pennsylvania 19104, USA

(Received 11 July 2007; published 6 March 2008)

We study the proximity effect between an s-wave superconductor and the surface states of a strong topological insulator. The resulting two-dimensional state resembles a spinless $p_x + ip_y$ superconductor, but does not break time reversal symmetry. This state supports Majorana bound states at vortices. We show that linear junctions between superconductors mediated by the topological insulator form a nonchiral one-dimensional wire for Majorana fermions, and that circuits formed from these junctions provide a method for creating, manipulating, and fusing Majorana bound states.

DOI: 10.1103/PhysRevLett.100.096407 PACS numbers: 71.10.Pm, 03.67.Lx, 74.45.+c, 74.90.+n

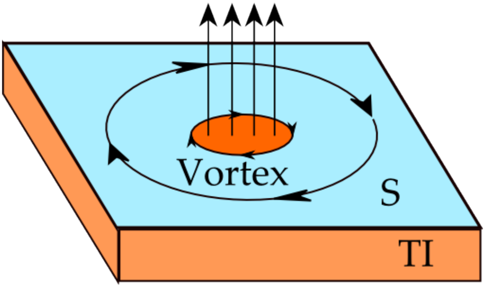

Majorana Modes: Topological Quantum Computing

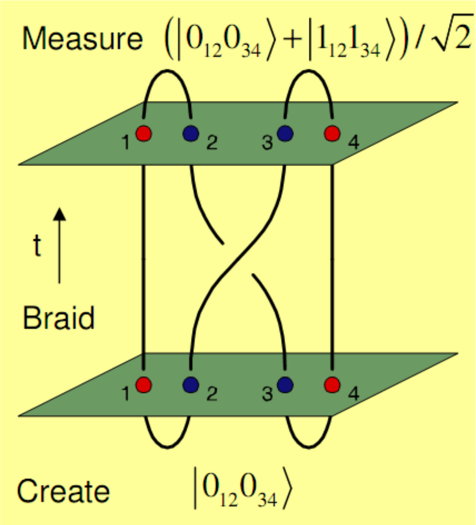

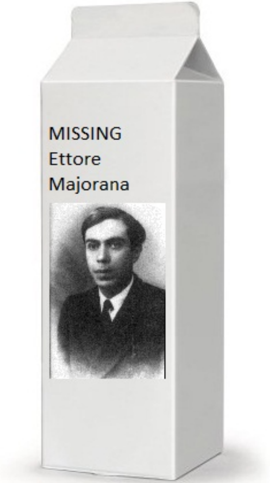

C. Kane - Exotic States of Matter Talk - Jan 14-2010

Fu-Kane Model (Phenomenological)

TI Surface Hamiltonian

$$h_s(\mathbf{k}) = -\mu_s + v_s(\sigma_x k_y - \sigma_y k_x),$$

Superconducting TI Surface Hamiltonian

$$H_{FK}(\mathbf{k}) = \begin{pmatrix} h_s(\mathbf{k}) & i\sigma_y \Delta_s \\ -i\sigma_y \Delta_s^* & -h_s^*(-\mathbf{k}) \end{pmatrix},$$

$$\mathbf{k} = (k_x, k_y),$$

Energy Dispersion

$$E(k) = \sqrt{|\Delta_s|^2 + (v_s k \pm \mu_s)^2}.$$

L. Fu and C. L. Kane, Phys. Rev. Lett. 100, 096407 (2008)

Goals

1) Verify Fu-Kane Model from self-consistent microscopic calculation
2) Order Parameter suppression
3) Triplet Pairing Correlations (due to SO Coupling)

Geometry

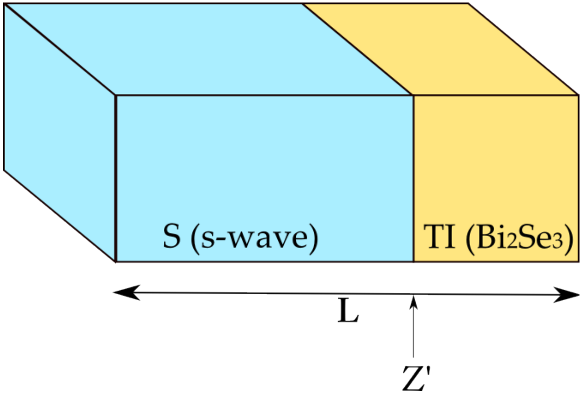

TI Model

Low energy $\mathbf{k}\cdot\mathbf{p}$ $\mathcal{H}$ in the basis $\{|1\uparrow\rangle, |1\downarrow\rangle, |2\uparrow\rangle, |2\downarrow\rangle\}$,

$$H_{TI}(\mathbf{k}) = \begin{pmatrix} M(\mathbf{k}) & 0 & A_1 k_z & A_2 k_- \\ 0 & M(\mathbf{k}) & A_2 k_+ & -A_1 k_z \\ A_1 k_z & A_2 k_- & -M(\mathbf{k}) & 0 \\ A_2 k_+ & -A_1 k_z & 0 & -M(\mathbf{k}) \end{pmatrix} - \mu \hat{I}.$$

$k_\pm = k_x \pm i k_y$,

.

$M(\mathbf{k}) = M - B_1 k_z^2 - B_2(k_x^2 + k_y^2)$, μ is variable.

.

H. Zhang et al, Nature Physics 5, 438 (2009)

Metal Model: Turn off SOC

$$M(\mathbf{k}) = M - B_1 k_z^2 - B_2(k_x^2 + k_y^2)$$

$$H_{Metal}(\mathbf{k}) =$$

$$\begin{pmatrix} M(\mathbf{k}) & 0 & 0 & 0 \\ 0 & M(\mathbf{k}) & 0 & 0 \\ 0 & 0 & -M(\mathbf{k}) & 0 \\ 0 & 0 & 0 & -M(\mathbf{k}) \end{pmatrix} - E_F$$

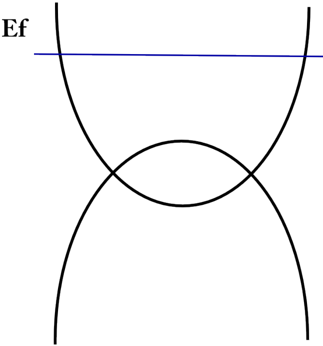

Then turn on superconductivity (Δ)...

Band Diagram

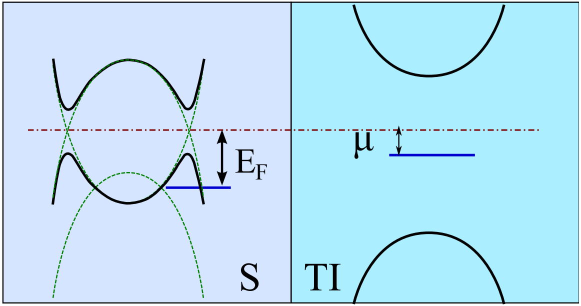

Superconducting gap $<<$ TI Insulating gap

BdG Hamiltonian

8×8 BdG Superconductor-TI Hamiltonian

$$\hat{H}_B = \begin{pmatrix} h_0 - \mu & \mathbf{d} \cdot \boldsymbol{\sigma} & 0 & 0 \\ \mathbf{d} \cdot \boldsymbol{\sigma} & -h_0 - \mu & 0 & -\Delta\, i\sigma_y \\ 0 & 0 & \mu - h_0 & \mathbf{d} \cdot \boldsymbol{\sigma}^* \\ 0 & \Delta^*\, i\sigma_y & \mathbf{d} \cdot \boldsymbol{\sigma}^* & \mu + h_0 \end{pmatrix}$$

$$d_x = A_1(z)k_x,\ d_y = A_1(z)k_y,\ d_z = A_2(z)(-i\partial_z),$$

$$h_0(\mathbf{k}_\parallel, \partial_z) = M - B_1\partial_z^2 - B_2 k_\parallel^2$$

Fourier Expansion

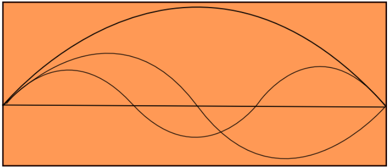

$$u_{n,l\sigma}(z) = \sum_m u_{nm}^{l\sigma}\,\phi_m(z), \quad v_{n,l\sigma}(z) = \sum_m v_{nm}^{l\sigma}\,\phi_m(z),$$

$$\Delta(z) = \sum_m \Delta_m\,\phi_m(z), \quad \phi_m(z) = \sqrt{2/L}\sin(k_m z).$$

BdG equation becomes an $8N \times 8N$ matrix equation.

.

K. Halterman and O. T. Valls, Phys. Rev. B 65, 014509 (2001)

Order Parameter Δ

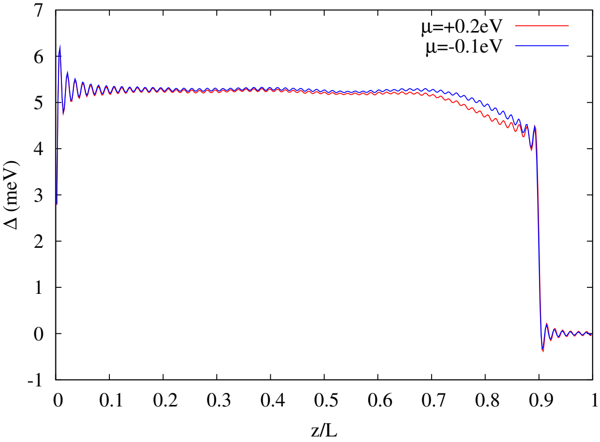

$\mu = -0.1\text{eV}$ (Blue) and $\mu = 0.2\text{eV}$ (Red)

$L = 160\text{nm}$, $\Delta_0 \sim 5.2\text{meV}$.

Triplet Correlations

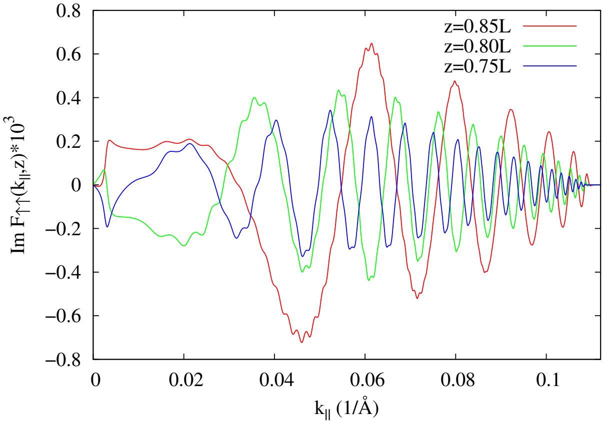

$\mathrm{Im}[F_{\uparrow\uparrow}(k_{\|}, z)]$: $d = 0.9L$, $\mu = 0$, $L = 160\text{nm}$, $\Delta_0 = 5.2\text{meV}$

T. D. Stanescu, et al, Phys. Rev. B 81, 241310 (2010)

A. M. Black-Schaffer, Phys. Rev. B 83, 060504 (2011)

Fu-Kane Model Verification

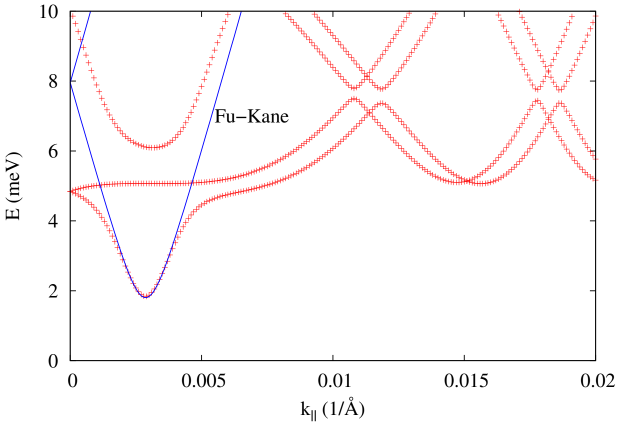

$\epsilon_n(k_{\|})$ $\mu = 0$, $L = 160$nm, Δ_0 ~5.2meV

Fu-Kane model fit: $\Delta_s = 1.8$meV, $v_s = 2.7$eVÅ, and $\mu_s = 7.5$meV

$$E(k) = \sqrt{|\Delta_s|^2 + (v_s k \pm \mu_s)^2}$$

Fu-Kane Model Verification - Vary μ

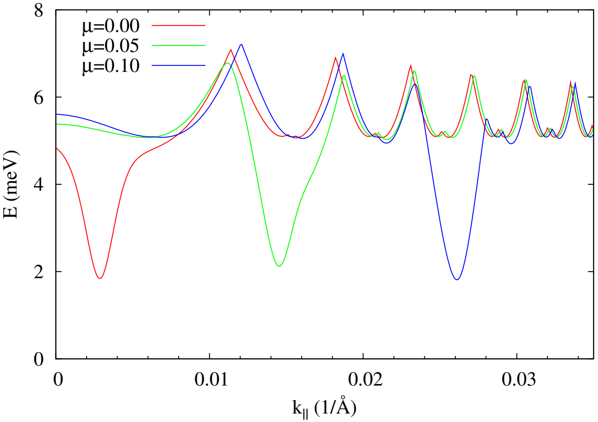

$L = 160\text{nm}$, $\Delta_0 \sim 5.2\text{meV}$

$\mu = \{.00, .05, .10\}\text{eV}$

Location of the Fu-Kane Modes

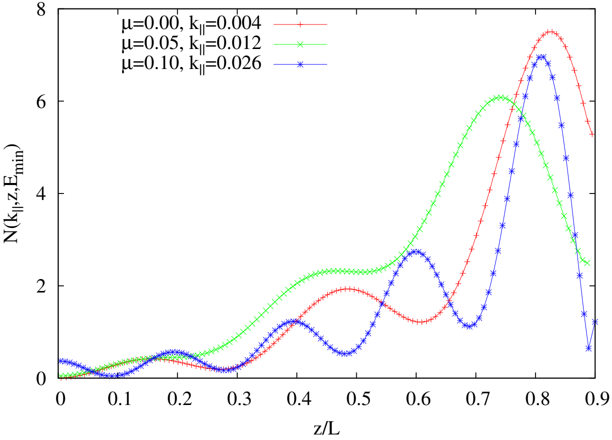

Envelope of $N(k_{||}, z, \omega)$, $\omega = E_{min}$
$z' = 0.9L$, L=160nm

Summary

Order parameter is mildly suppressed
Induced triplet pairing correlations due to SO coupling
Interface modes below the bulk superconducting gap
$\rightarrow$ Fu-Kane Model verified, parameters renormalized.

Understanding the bulk effects of the TI are great.
How about the surface?

Superconducting Josephson Junction Surface

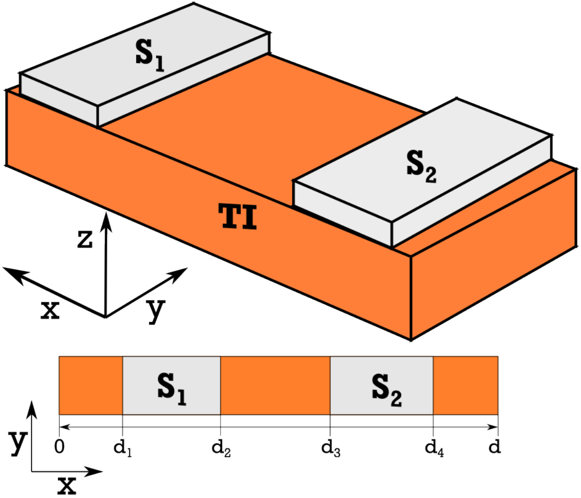

S_1 and S_2 are the two superconducting leads (Sn, Pb, Al, etc.)

Model and Basic Equations

Surface Dirac-Bogoliubov-de Gennes Hamiltonian,

$$\mathcal{H} = \begin{pmatrix} h_+ & \hat{\Delta} \\ \hat{\Delta}^\dagger & h_- \end{pmatrix}, \tag{1}$$

where

$$h_\pm = -i\hbar v_F(\sigma_x\partial_x \pm \sigma_y\partial_y) \mp \mu(x), \tag{2}$$

$$\hat{\Delta} = i\sigma_y\Delta(x). \tag{3}$$

The basis

$$\psi_n = \left(u_{n\uparrow}, u_{n\downarrow}, v_{n\uparrow}, v_{n\downarrow}\right)^T, \tag{4}$$

which satisfies $\mathcal{H}\psi_n = \epsilon_n\psi_n$, represents the BdG particle $(u_\sigma(k_y, x))$, and hole $(v_\sigma(k_y, x))$

Model and Basic Equations

Initial order parameter and chemical potential:

$$\Delta(x) = \begin{cases} \Delta_0, & (d_1 < x < d_2) \\ \Delta_0 e^{i\phi}, & (d_3 < x < d_4) \\ 0, & \text{elsewhere} \end{cases}, \tag{5}$$

$$\mu(x) = \begin{cases} \mathcal{E}_F, & (d_1 < x < d_2) \text{ or } (d_3 < x < d_4) \\ \mu, & \text{elsewhere} \end{cases}, \tag{6}$$

Gap equation

$$\Delta(x) = g(x) \int dk_y {\sum_n}' u_{n\uparrow}(k_y, x) v^*_{n\downarrow}(k_y, x) \tag{7}$$

$g(x)$: contact pairing potential

$$g(x) = \begin{cases} g_0, & (d_1 < x < d_2) \text{ or } (d_3 < x < d_4) \\ 0, & \text{elsewhere} \end{cases} \tag{8}$$

Model and Basic Equations

This basis expansion results in a 4N $\times$ 4N matrix Hamiltonian of:

$$\mathcal{H} = \begin{pmatrix} -\mu_{nm} & \mathcal{K}^{-}_{nm} & 0 & \hat{\Delta}_{nm} \\ \mathcal{K}^{+}_{mn} & -\mu_{nm} & -\hat{\Delta}_{nm} & 0 \\ 0 & -\hat{\Delta}^{*}_{nm} & \mu_{nm} & \mathcal{K}^{+}_{nm} \\ \hat{\Delta}^{*}_{nm} & 0 & \mathcal{K}^{-}_{mn} & \mu_{nm} \end{pmatrix}, \tag{9}$$

with

$$\mathcal{K}^{\pm}_{nm} = -i\hbar v_F (k_m B_{nm} \pm k_y \delta_{nm}), \tag{10}$$

$$B_{nm} = \frac{2}{d}\int_0^d \sin(k_n x)\cos(k_m x)dx \tag{11}$$

$$\mu_{nm} = \frac{2}{d}\int_0^d \mu(x)\sin(k_n x)\sin(k_m x)dx \tag{12}$$

$$\hat{\Delta}_{nm} = \frac{2}{d}\int_0^d \Delta(x)\sin(k_n x)\sin(k_m x)dx \tag{13}$$

in the basis of

$$\psi = (u_{n\uparrow 1}\ldots u_{n\uparrow N}, u_{n\downarrow 1}\ldots u_{n\downarrow N}, v_{n\uparrow 1}\ldots v_{n\uparrow N}, v_{n\downarrow 1}\ldots v_{n\downarrow N},)^T,$$

Energy Spectrum: Zero Bias Junction

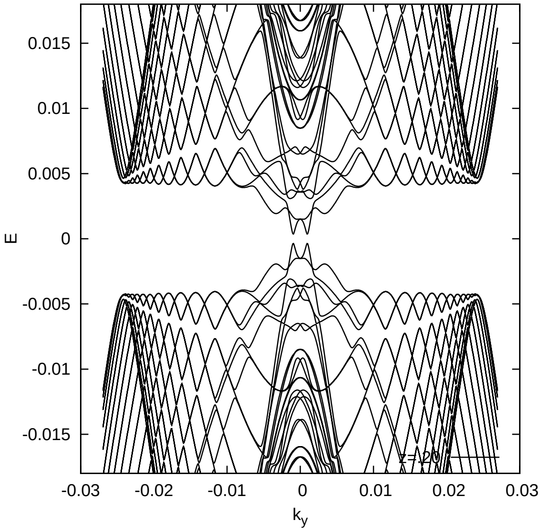

Figure: Energy spectrum of zero-bias (left) and pi-bias (right) junction. TI chemical potential is set to 5 meV. Energy in units of eV.

Energy Spectrum: π Bias Junction

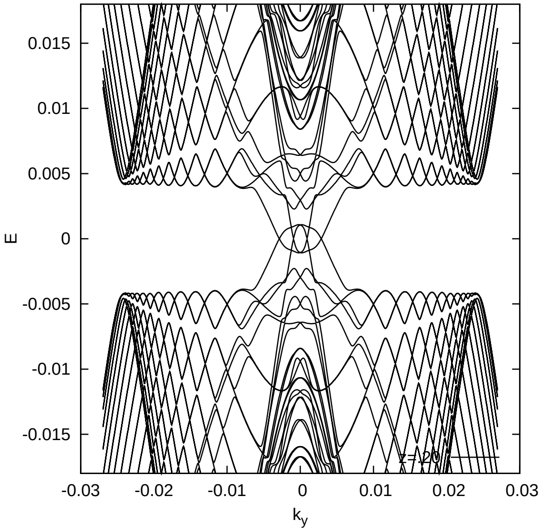

Figure: Energy spectrum of zero-bias (left) and pi-bias (right) junction. TI chemical potential is set to 5 meV. Energy in units of eV.

Order Parameter and Singlet Correlation

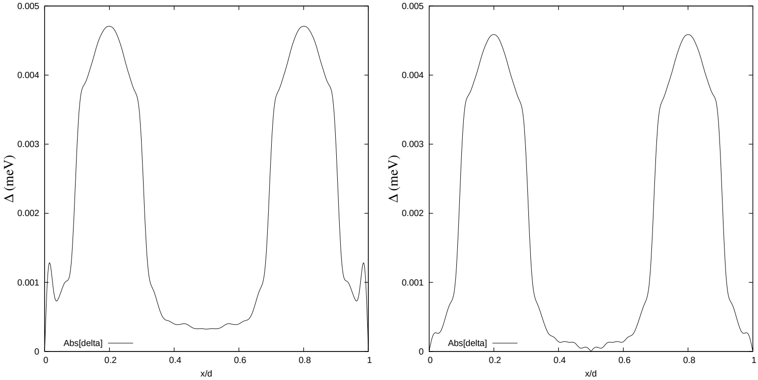

Figure: The absolute value of the singlet correlation profiles of the zero (left) and π (right) junctions. The π junction falls to zero at the midpoint. The left side of the midpoint is positive valued while the right side is negative valued. Energy of the order parameter is measured in eV and x/d is the unit-less relative distance along the structure.

Local Density of States: Zero Bias Junction

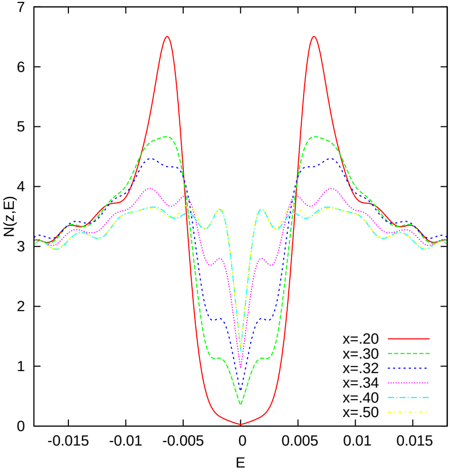

Figure: Local density of states at different positions in the heterostructure. Left (right) is the zero (π) biased junction. Energy in units of eV.

Local Density of States: π Junction

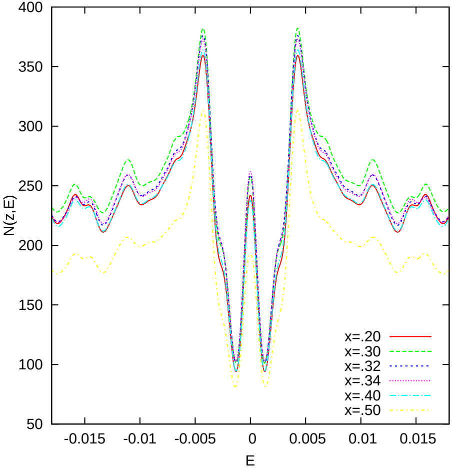

Figure: Local density of states at different positions in the heterostructure. Left (right) is the zero (π) biased junction. Energy in units of eV.

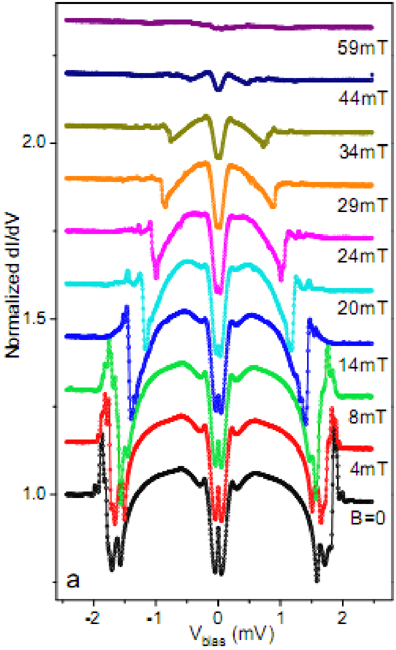

59mT
44mT
34mT
29mT
24mT
20mT
14mT
8mT
4mT
B=0
a
Normalized dI/dV
2.0
1.5
1.0
-2
-1
0
1
2
V_{bias} (mV)

Spectral Function

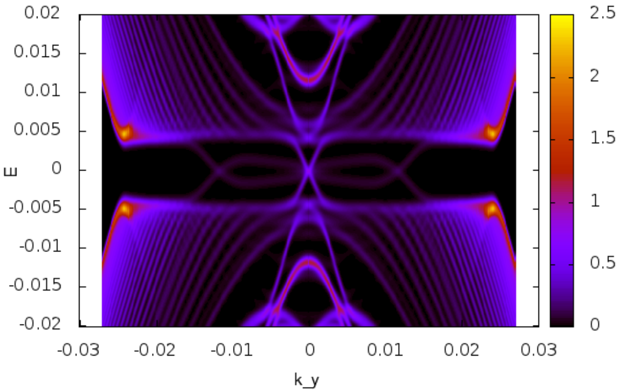

Figure: Local spectral function near the midpoint ($\approx .55$) of the π junction heterostructure. Energy in units of eV. k_y in units of $Å^{-1}$

TI-FET: MOSFET with a Topological Insulator

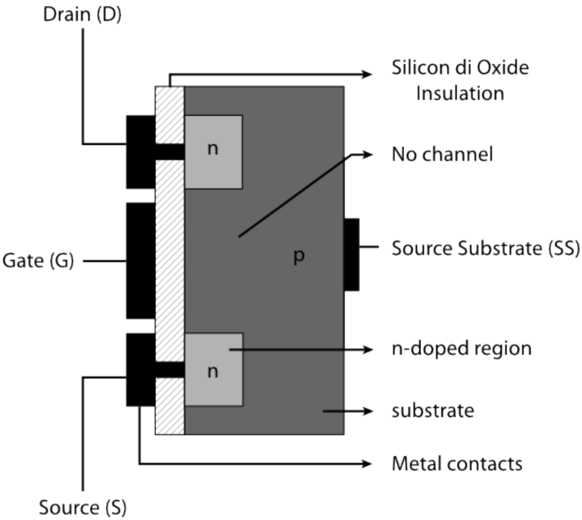

Figure: (left) A proposed heterostructure that exploits the exotic surface states that differ from the bulk in a TI. (right) A typical n-type MOSFET.

MOSFET

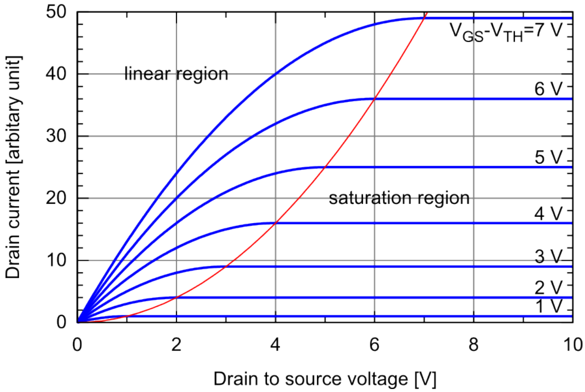

Figure: (left) A proposed heterostructure that exploits the exotic surface states that differ from the bulk in a TI. (right) A typical n-type MOSFET.

TI as the Floating Gate

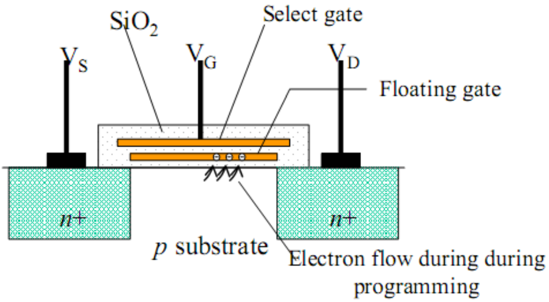

Figure: A floating gate MOSFET. The main difference seen here is the additional “programming gate” above the voltage gate normally seen in a MOSFET.

TI as the current channel

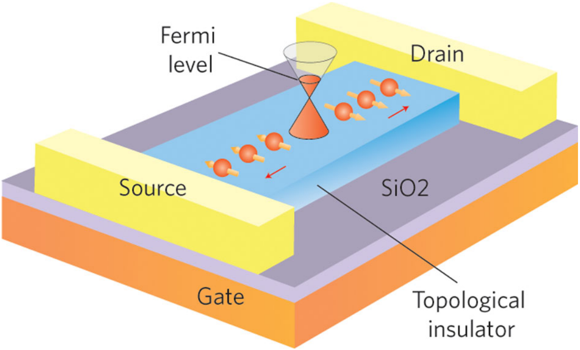

Figure: (left) A proposed heterostructure that exploits the exotic surface states that differ from the bulk in a TI. (right) A typical n-type MOSFET.

Summary

Thank you!